Probiotics and Antimicrobial Proteins
https://doi.org/10.1007/s12602-025-10773-2

RESEARCH

Therapeutic Potential and Sustainable Bioprocessing of Enterocin CC2: A Probiotic-Derived Antimicrobial Targeting *Streptococcus mutans* in Oral Health

Zhang Jin Ng[1] · Chee-Yuen Gan[2] · Mazni Abu Zarin[3] · Chee Keong Lee[1] · John Chi-Wei Lan[4] · Hui Suan Ng[5,6] · Joo Shun Tan[1]

Received: 19 June 2025 / Accepted: 8 September 2025

Abstract

The growing threat of antimicrobial resistance in oral pathogens necessitates safe and sustainable alternatives to conventional therapies. Enterocin CC2, a novel bacteriocin from *Enterococcus faecium* CC2, was purified using an optimized polyethylene glycol (PEG)–citrate aqueous two-phase system (ATPS). The process achieved a purification factor of 4.73 and recovery yield of 73.33%, which improved to 5.13 and 84.61% with the addition of 4% NaCl. SDS-PAGE revealed a molecular size of ~ 5.5–6 kDa, and identity confirmation was obtained via HPLC and LC–MS. Enterocin CC2 displayed potent antimicrobial activity against *Streptococcus mutans* with MIC and MBC values of 0.50 and 1.00 mg/mL, respectively, and demonstrated faster bactericidal action than 0.2% chlorhexidine. ISO 10993–5 cytotoxicity testing confirmed its safety on 3T3-L1 cells at concentrations ≤ 1 mg/mL. These findings highlight enterocin CC2 as a promising candidate for oral health applications and establish PEG–citrate ATPS as a scalable, eco-friendly platform for bacteriocin purification.

Keywords Enterocin CC2 · Probiotic-derived antimicrobial · Oral health therapeutics · Bacteriocin purification · PEG-based aqueous two-phase system · *Streptococcus mutans*

Introduction

Dental caries remains one of the most widespread chronic infectious diseases globally, affecting nearly 2 billion adults and more than 500 million children according to the World Health Organization [22]. This multifactorial condition is primarily driven by acidogenic bacteria, with *Streptococcus mutans* recognized as the principal etiological agent [7]. By metabolizing dietary carbohydrates—especially sucrose—into organic acids, *S. mutans* lowers the local pH and demineralizes dental enamel, initiating caries development (Zhang Jin [17]). Its high aciduricity, robust biofilm-forming ability, and persistence within the extracellular polysaccharide matrix of dental plaque contribute to its dominance in cariogenic environments [14].

Conventional strategies for controlling *S. mutans*, such as broad-spectrum antibiotics (e.g., penicillin, tetracycline) and chemical antiseptics (e.g., chlorhexidine), are increasingly limited by rising antimicrobial resistance (AMR), disruption of commensal microbiota, and side effects including mucosal irritation, altered taste, and tooth staining [2]. The global AMR crisis has therefore accelerated interest

✉ Joo Shun Tan
jooshun@usm.my

1 Bioprocess Technology, School of Industrial Technology, Universiti Sains Malaysia, 11800 Gelugor, Pulau Pinang, Malaysia

2 Analytical Biochemistry Research Centre (ABrC), University Innovation Incubator Building, Universiti Sains Malaysia, Sains@USM Campus, 11900 Bayan Lepas , Penang, Malaysia

3 Laboratory Vaccines and Biomolecules, Institute of Bioscience, Universiti Putra Malaysia, UPM Serdang, 43400 Serdang, Selangor, Malaysia

4 Biorefinery and Bioprocessing Engineering Laboratory, Department of Chemical Engineering and Materials Science, Yuan Ze University, Chungli, Taoyuan 320, Taiwan

5 Department of Chemical Engineering and Materials Science, Yuan Ze University, Chungli, Taoyuan 320, Taiwan

6 Smart Bioresource Recovery and Formulation Laboratory, Department of Chemical Engineering and Materials Science, Yuan Ze University, Chungli, Taoyuan 320, Taiwan

Published online: 18 September 2025

in precision-targeted antimicrobials derived from probiotic microorganisms [19]. Recent genomic and functional profiling of probiotic strains, such as *Lactiplantibacillus plantarum* K25, has further highlighted their diverse probiotic mechanisms and bioactivities, strengthening the rationale for bacteriocin-based therapeutics [3].

Among these, bacteriocins—ribosomally synthesized antimicrobial peptides produced by lactic acid bacteria (LAB)—have gained considerable attention due to their selective pathogen inhibition, probiotic origin, and minimal toxicity. Enterocins, in particular, exhibit broad-spectrum antimicrobial activity and stability, with *Enterococcus faecium* CC2 identified as a promising LAB strain capable of producing enterocin CC2, a novel bacteriocin with potent inhibitory activity against *S. mutans* and *Candida albicans*, both of which contribute to polymicrobial biofilm-associated oral infections (Zhang Jin [17]). In parallel, comprehensive genomic analysis of *Pediococcus acidilactici* BCB1H underscores the broader biotechnological and health relevance of bacteriocin-producing LAB [4, 5].

Despite their therapeutic potential, the clinical translation of bacteriocins is hindered by the complexity and cost of downstream purification. Chromatographic techniques, although effective, are expensive, labor-intensive, and often account for up to 80% of total production costs [15]. Therefore, the development of scalable, sustainable, and biocompatible purification methods is critical to advance probiotic-derived antimicrobials into practical applications [11]. Aqueous two-phase systems (ATPS), particularly PEG–salt-based systems, have emerged as eco-friendly, cost-effective, and biocompatible platforms for biomolecule recovery [24]. ATPS provides selective partitioning, scalability, and alignment with green manufacturing principles, and recent studies have confirmed its success in purifying enzymes, proteins, and bioactives from microbial sources [6]. Concurrently, advances in peptide characterization and microbiological methods—such as recent work on *Lactiplantibacillus plantarum* NMGL2—enable more robust validation of bacteriocin purity, structure, and bioactivity, further facilitating translational applications [4, 5].

Building on these advances, the present study investigates the sustainable bioprocessing of enterocin CC2 using an optimized PEG–citrate ATPS. By systematically varying PEG concentration, crude load, pH, salt type, and temperature, the process was optimized to maximize purification efficiency while preserving antimicrobial bioactivity. Furthermore, the antimicrobial potency of enterocin CC2 against *S. mutans* was evaluated, alongside biosafety testing according to ISO 10993–5 cytotoxicity standards. Collectively, this work advances the translational development of probiotic-derived bacteriocins as safe, targeted, and sustainable alternatives for oral healthcare, directly addressing the urgent need for novel strategies to combat AMR in dentistry.

Materials and Methods

Cultivation of *Enterococcus faecium* CC2 and Recovery of Crude Bacteriocin-Containing Supernatant

Enterococcus faecium CC2 was cultivated in de Man, Rogosa and Sharpe (MRS) broth (Merck, Darmstadt, Germany) at 37 °C for 24 h under static conditions to promote optimal bacteriocin production. Following incubation, the cultures were centrifuged at 9000 rpm for 15 min at 4 °C to pellet the bacterial cells (Z. J. [17]). The resulting cell-free supernatant, containing the extracellular bacteriocin, was carefully collected and subjected to purification using an aqueous two-phase system (ATPS).

Construction of Binodal Curves

To evaluate the phase-forming behaviour of the aqueous two-phase system (ATPS), sodium citrate was selected as the salt phase due to its biocompatibility and minimal interference with bacteriocin activity across a broad concentration range. Crude bacteriocin-containing extract from *E. faecium* CC2 was first subjected to 80% ammonium sulphate saturation to concentrate and partially purify the protein content. The resulting precipitate was collected, redissolved, and subsequently introduced into the ATPS.

Binodal curves, which delineate the boundary between monophasic and biphasic regions, were constructed to determine the phase separation capability of sodium citrate in combination with polyethylene glycol (PEG) of varying molecular weights (PEG 2000, 4000, 6000, and 8000). The turbidimetric titration method described by Hatti-Kaul was employed for this purpose. Sixteen turbid mixtures were prepared by combining varying concentrations of PEG and sodium citrate in 5 g ATPS systems. Distilled water was incrementally added to each mixture until turbidity disappeared, indicating the transition to a one-phase system. The volume of distilled water required to reach this point was recorded, and the corresponding PEG and salt concentrations were used to calculate the final composition.

These critical data points were plotted to generate binodal curves for each PEG–sodium citrate combination, facilitating the selection of optimal systems for downstream partitioning of enterocin CC2 [20].

ATPS Factor Screening Using Full Factorial Design

Various ATPS compositions were screened by mixing specific volumes of PEG and sodium citrate solutions in 15 mL tubes, followed by the addition of the crude bacteriocin extract. Each formulation was adjusted to 5 g with distilled water, vortexed, and centrifuged at 3500 rpm for

10 min. Both phases were dialyzed (3.5 kDa MWCO) for 6 h with buffer changes every 2 h to remove residual salts. A two-level full factorial design (Design Expert v7.0) was employed to examine the influence of five variables—crude load (5–15%, w/w), pH (4–10), PEG concentration (10–20%, w/w), salt concentration (10–15%, w/w), and temperature (25–55 °C)—on purification factor, recovery yield, and partition coefficient. Ninety-nine experimental runs were performed, including replicates and center points.

Optimization Using Central Composite Design (CCD)

Response surface methodology (RSM) with central composite design (CCD) was used to optimize the ATPS conditions. The five significant factors identified were modeled using polynomial regression to evaluate their effects and interactions on recovery yield, purification factor, and partition coefficient. The design identified optimal purification conditions with maximal efficiency. The observed responses from CCD design were then fitted to the following polynomial Eq. 7 below:

$$Y = \beta_0 + \sum_{i=1}^{k} \beta_i x_i + \sum_{i=1}^{k} \beta_{ii} x_i^2 + \sum_{i=1}^{k} \sum_{j=1}^{k} \beta_{ij} x_i \beta_{ii} x_j + \varepsilon \quad (1)$$

where Y represents predicted response; *i* and *j* represent the index numbers for the pattern; β represents the offset term; β*i*, β*ii*, and β*ij* represent the coefficients for the linear, quadratic, and interaction effects, respectively; *xi* and *xj* represent the coded variables; and ε represents the error. After the optimization, the composition of PEG, crude loading and sodium citrate concentration with highest desirability in purification factor, recovery yield and partition coefficient at fixed pH and temperature could be achieved [21].

Antimicrobial Assay

S. mutans UKMCC1019 was cultured in Brain Heart Infusion (BHI) broth at 37 °C for 24 h, and the optical density (OD) of the cell culture was diluted to 0.03. Subsequently, 100 µL of the cell suspension was evenly spread on yeast malt agar and allowed to dry. Holes were then made in each quadrant of the agar, and 100 µL of supernatant containing bacteriocin was added to each well. Streptomycin (10 mg/mL; Bio Basic, Canada) was used as a positive control. The plates were then incubated at 37 °C for 24 h, and bacteriocin activity was determined using the following equation:

$$\text{Bacteriocin activity} = \frac{L_z - L_S}{V} \quad (2)$$

where L_z represents the clear zone area (mm^2), *Ls* represents well area (mm^2) and V represents volume of the sample (mL).

Protein Quantification

Protein concentration was measured using the Bradford method. Briefly, a total of 200 µL of diluted Bradford reagent (Bio-Rad, USA) and 10 µL of the sample were added to individual wells in a 96-well microtiter plate. The plate was then incubated at 37 °C for 10 min. Following incubation, absorbance was measured at 595 nm. The protein content in the sample was quantified by comparing the absorbance values to a standard curve of protein concentration, with bovine serum albumin (BSA) serving as the reference standard.

Purification Performance Calculations

The following formulas were used to determine the bacteriocin specific activity (SA), partition coefficient (K), recovery yield (Y), and purification factor (PF):

$$\text{SA (AU / mg)} = \frac{\text{bacteriocin activity, AU/mL}}{\text{[Protein], mg/mL}} \quad (3)$$

$$\text{Purification factor} = \frac{\text{SA of bacteriocin in top phase/supernatant/ precipitate}}{\text{SA of crude bacteriocin}} \quad (4)$$

$$\text{Recovery yield (\%)} = \frac{\text{bacteriocin activity in top phase/supernatant/ precipitate}}{\text{Crude bacteriocin activity}} \text{ x } 100 \quad (5)$$

$$\text{Partition coefficient, K} = \frac{\text{bacteriocin activity in the top phase}}{\text{bacteriocin activity in the bottom phase}} \quad (6)$$

Sodium Dodecyl Sulphate–polyacrylamide Gel Electrophoresis (SDS-PAGE) Analysis

Protein precipitation step was performed with acetone prior to SDS-PAGE analysis. The size of bacteriocin was determined by SDS-PAGE analysis with 15% (v/v) of resolving gel and 4% (v/v) of stacking gel. The process was carried out with

Mini-Vertical SE250 electrophoresis unit (Amersham Biosciences, USA) at 110 V for 95 min. Then, the staining of the gel was done by using Page Blue Protein Staining Solution (Thermo Fisher Scientific, USA), followed by de-staining by using deionized water. The size of the bacteriocin was observed by comparing to protein standard size marker (Sigma Aldrich, USA) [12].

High-performance Liquid Chromatography (HPLC) Characterization

The crude and partially purified bacteriocin underwent analysis via HPLC utilizing a C18 column [18]. The samples were subjected to elution using two mobile phases: mobile phase A, consisting of 99.9% water and 0.1% trifluoroacetic acid (TFA) (Merck, Darmstadt, Germany), and mobile phase B, comprising 99.9% acetonitrile (ACN) (Merck, Darmstadt, Germany) and 0.1% TFA. Elution was conducted at a flow rate of 0.5 mL/min, with the mobile phase composition transitioning as follows: 90% A and 10% B for 0–5 min, 50% A and 50% B for 5–30 min, 20% A and 80% B for 30–35 min, 10% A and 90% B for 35–50 min, and finally 90% A and 10% B for 50–60 min. Peak detection was performed at 280 nm. Fractions collected from the partially purified bacteriocin were assessed for their antimicrobial activities, and the fraction exhibiting inhibitory effects was selected for freeze-drying.

Liquid chromatography–mass Spectrometry (LC–MS) Identification

The freeze-dried bacteriocin was resuspended in a solution of 0.1 M ammonium bicarbonate (Sigma Aldrich, USA) and 1 M urea (Sigma Aldrich, USA). After that, reduction and alkylation of the bacteriocin were carried out by adding 50 mM tris(2-carboxyethyl) phosphine (Sigma Aldrich, USA) and 150 mM iodoacetamide (Bio-Rad, USA), respectively, to the bacteriocin suspension, followed by the addition of 1% (w/w) of sodium deoxycholate (Thermo Scientific, MA, USA). Then, 4 µg of trypsin (Promega, Madison, WI, USA) in 50 mM NH4HCO3 was added and the solution was incubated at 37˚C for 16 h. After 16 h, the sample was centrifuged at 14 000 g for 15 min and sodium deoxycholate was discharged. The sample was dried by using centrifugal evaporator. 30 µL of solution containing 0.1% formic acid (FA) (Merck, Darmstadt, Germany) and 5% ACN was added to the sample, followed by the loading of 2 µL of into Acclaim PepMap 100 C18 column (2 µm, 0.075 × 150 mm) (Thermo Scientific, MA, USA). Mobile phases A and B used in this system were 0.1% of FA and 80% of ACN containing 0.1% FA, respectively. Sample elution was conducted at gradient of 5–35% mobile phase B in 75 min and flow rate of 300 nL/min. EASY-nano liquid chromatography (EASYnLC) 1200 System (Thermo Scientific, MA, USA) was used to separate the peptides in the system, while peptide ions was generated by using Q Exactive Plus Hybrid Quadrupole-Orbitrap mass spectrometer system (Thermo Scientific, MA, USA). Precursor ion scan was carried out with the settings of 70,000 of resolution and of 310–1800 m/z of mass range [13].

Minimum Inhibitory Concentration (MIC) & Minimum Bactericidal Concentration (MBC) Determination

The minimum inhibitory concentration (MIC) and minimum bactericidal concentration (MBC) of the partially purified bacteriocin on *S. mutans* UKMCC1019 was determined by using 96 well microtiter plate method and viable cells count method, respectively. Two-fold dilution of the bacteriocin was done from column to column and the turbidity of the samples were measured as the absorbance at 596 nm after 24 h. The column without bacteriocin was used as control in this assay. The percentage of growth inhibition of partially purified bacteriocin against *S. mutans* UKMCC1019 was calculated by using the following equation [9]:

$$\text{Percentage of inhibition, } \% = \frac{OD_{control} - OD_{sample}}{ODcontrol} \times 100 \quad (7)$$

where OD control represents the changes in optical density of the growth control and OD sample represents the changes in the optical density of the sample.

The MIC was defined as the lowest bacteriocin concentration that entirely inhibited the *S. mutans* UKMCC1019 by calculating the percentage of inhibition, whereas MBC was determined as a lowest concentration of the partially purified bacteriocin that killed *S. mutans* UKMCC1019 completely by viable cells count method [16].

Growth Curve and Time-kill Kinetics

For growth curve assay, the overnight culture of *S. mutans* UKMCC1019 was inoculated anaerobically to exponential phase with a fresh BHI medium and 1 × MIC (0.500 mg/mL) of partially purified bacteriocin was added. Samples were collected for every hour until stationary phase of growth of *S. mutans* UKMCC1019 and dry cell weight of samples were measured and recorded. In this assay, *S. mutans* UKMCC1019 culture without partially purified bacteriocin was used as negative control, while 0.2% of chlorhexidine (Supelco, USA) was used as a positive control. The test was performed with triplicate samples [25].

For time-kill kinetics assays, the *S. mutans* UKMCC1019 suspension was adjusted to 1×10^7 CFU/mL. After that, the partially purified bacteriocin with concentrations of 1-, 2- and fourfold of the MBC was added, respectively. The suspensions

were incubated at 37 °C for 24 h and the samples were collected for every hour, followed by viable cell count using BHI agar. In this assay, *S. mutans* UKMCC1019 culture without partially purified bacteriocin was used as negative control, while 0.2% of chlorhexidine was used as a positive control. The test was performed with triplicate samples [8].

Cytotoxicity Assay

The cytotoxic effect of the partially purified enterocin CC2 was evaluated against 3T3-LI (normal cell) by MTT [3-(4,5-dimethyl-2-thiazolyl)−2,5-diphenyl-2H-tetrazolium bromide] (Sigma Aldrich, USA) assay [23]. In brief, seeded cells were treated with 2 to 0.125 mg/ml samples and incubated for 24 h. Untreated cells were used as the negative control. After incubation, cells were incubated with MTT at 37 °C for 4 h. Then, dimethyl sulfoxide (DMSO) (Sigma Aldrich, USA) was added to dissolve MTT-formazan crystals, and the absorbance was measured at 540 nm with 620 nm as a reference by a microplate reader. The test was performed with triplicate samples. The percentage of cell viability was determined according to the following equation [10]:

$$\text{Percentage of cell survival, } \% = \frac{\textit{Absorbance in treated wells}}{\textit{Absorbance in negative control well}} \text{x } 100 \tag{8}$$

Results and Discussion

Optimization of ATPS for Bacteriocin Purification

The precipitate obtained after ammonium sulphate saturation was further purified using an aqueous two-phase system (ATPS) composed of PEG and sodium citrate, with the phase composition determined based on the constructed binodal curve (Fig. S1).

Statistical analysis using ANOVA indicated that the two-level full factorial models for purification factor (PF), recovery yield (Y), and partition coefficient (K) were statistically significant (Table S1). Following the screening results, optimization was performed using a central composite design (CCD), varying key parameters: crude loading (8–12% w/w), pH (6–8), PEG 6000 concentration (13–17% w/w), sodium citrate concentration (11.5–13.5% w/w), and temperature (35–45 °C).

As shown in Table 1, the optimal purification conditions yielded a purification factor of 4.73, a recovery yield of 73.33%, and a partition coefficient of 5.63. These results were achieved using an ATPS composition of 10% (w/w) crude loading, 15% (w/w) PEG 6000, and 12.50% (w/w) sodium citrate at pH 7 and 40 °C. The ANOVA results further validated the model's significance in describing the relationship between the selected factors and purification responses (Table 2). The final regression equations in coded factors for PF, Y, and K were derived as follows:

$$\begin{aligned} PF = {} & 4.592 + 0.078A + 0.11B - 0.099AD \\ & - 0.13AE\ 0.17BC + 0.14BE + 0.14CD \\ & + 0.089DE \end{aligned} \tag{9}$$

$$\begin{aligned} Y = {} & 71.30 + 1.23\ A + 1.71B - 1.57AD \\ & - 1.92AE - 2.62BC + 2.16BE + 2.21CD \\ & + 1.41DE \end{aligned} \tag{10}$$

$$\begin{aligned} K = {} & 5.50 + 0.071A + 0.11B - 0.098AD \\ & - 0.13AE - 0.17BC + 0.14BE + 0.14CD \\ & + 0.087DE \end{aligned} \tag{11}$$

The impact of NaCl concentration (1–6% w/w) on the purification of bacteriocin using ATPS was evaluated. As shown in Fig. 1, the addition of 4% (w/w) NaCl significantly enhanced the purification factor (PF), recovery yield (Y), and partition coefficient (K), reaching values of 5.134, 84.614%, and 6.374, respectively. The presence of NaCl increased the electrical potential difference between the phases, thereby facilitating the preferential partitioning of bacteriocin molecules into the PEG-rich top phase. However, at higher NaCl concentrations (5–6% w/w), a decline in bacteriocin activity and stability was observed. This may be attributed to the competitive migration of impurities into the PEG-rich phase, reducing available space and driving bacteriocin molecules into the salt-rich phase.

For comparison, Abdul Aziz et al. [1] employed an aqueous impregnated resin system (AIRS) using PEG-impregnated Amberlite XAD-4 and reported a maximum PF of 3.26 with a recovery yield of 82.69% ± 0.06% under optimized conditions [1]. While the yield obtained in that study is comparable, the higher PF achieved in the present work clearly demonstrates the improved purification efficiency and selectivity of the PEG–citrate ATPS. Importantly, this system operates under mild and biocompatible conditions, thereby preserving bacteriocin bioactivity while enhancing recovery.

The superior performance of the PEG–citrate ATPS established here underscores its potential as a practical bioprocessing strategy for probiotic-derived antimicrobials. Its non-denaturing nature, operational simplicity, and scalability make it a promising platform for downstream processing of sensitive bioactives such as bacteriocins intended for therapeutic applications.

Table 1 Actual and predicted purification factor, recovery yield and partition coefficient of bacteriocin

No	Crude Loading, pH w/w%		PEG 6000 concentration, w/w %	Sodium citrate concentration, w/w %	Temperature, °C	Purification Factor		Yield, %		Partition Coefficient, K	
						Actual	Predicted	Actual	Predicted	Actual	Predicted
1	8.00	6.00	13.00	11.50	35.00	2.84	3.00	44.02	46.57	3.74	3.91
2	12.00	6.00	13.00	11.50	35.00	3.35	3.47	51.94	53.73	4.25	4.36
3	8.00	8.00	13.00	11.50	35.00	3.37	3.40	52.24	52.76	4.27	4.30
4	12.00	8.00	13.00	11.50	35.00	3.9	3.90	60.45	60.50	4.8	4.80
5	8.00	6.00	17.00	11.50	35.00	2.68	2.80	41.54	43.39	3.58	3.72
6	12.00	6.00	17.00	11.50	35.00	3.45	3.53	53.48	54.70	4.35	4.43
7	8.00	8.00	17.00	11.50	35.00	2.53	2.54	39.23	39.37	3.43	3.45
8	12.00	8.00	17.00	11.50	35.00	3.32	3.31	51.46	51.25	4.24	4.21
9	8.00	6.00	13.00	13.50	35.00	2.83	2.83	43.87	43.90	3.75	3.75
10	12.00	6.00	13.00	13.50	35.00	2.91	2.87	45.11	44.55	3.83	3.78
11	8.00	8.00	13.00	13.50	35.00	3.04	2.93	47.12	45.49	3.94	3.84
12	12.00	8.00	13.00	13.50	35.00	3.13	3.01	48.53	46.71	4.05	3.93
13	8.00	6.00	17.00	13.50	35.00	3.24	3.21	50.22	49.83	4.16	4.13
14	12.00	6.00	17.00	13.50	35.00	3.57	3.52	55.35	54.63	4.47	4.42
15	8.00	8.00	17.00	13.50	35.00	2.77	2.66	42.96	41.20	3.67	3.57
16	12.00	8.00	17.00	13.50	35.00	3.12	3.00	48.36	46.57	4.02	3.91
17	8.00	6.00	13.00	11.50	45.00	2.76	2.86	42.78	44.32	3.66	3.77
18	12.00	6.00	13.00	11.50	45.00	2.78	2.84	43.09	44.04	3.68	3.73
19	8.00	8.00	13.00	11.50	45.00	3.84	3.83	59.52	59.38	4.74	4.74
20	12.00	8.00	13.00	11.50	45.00	3.88	3.85	60.14	59.68	4.78	4.75
21	8.00	6.00	17.00	11.50	45.00	2.62	2.68	40.61	41.49	3.54	3.60
22	12.00	6.00	17.00	11.50	45.00	2.87	2.93	44.49	45.35	3.77	3.82
23	8.00	8.00	17.00	11.50	45.00	3	2.99	46.5	46.33	3.9	3.91
24	12.00	8.00	17.00	11.50	45.00	3.3	3.28	51.15	50.77	4.2	4.18
25	8.00	6.00	13.00	13.50	45.00	3.11	3.07	48.23	47.54	4.01	3.98
26	12.00	6.00	13.00	13.50	45.00	2.69	2.63	41.69	40.75	3.59	3.53
27	8.00	8.00	13.00	13.50	45.00	3.87	3.74	59.99	58.00	4.77	4.65
28	12.00	8.00	13.00	13.50	45.00	3.48	3.34	53.94	51.78	4.4	4.25
29	8.00	6.00	17.00	13.50	45.00	3.52	3.47	54.56	53.82	4.42	4.39
30	12.00	6.00	17.00	13.50	45.00	3.36	3.30	52.08	51.17	4.26	4.20
31	8.00	8.00	17.00	13.50	45.00	3.63	3.49	56.28	54.06	4.55	4.40
32	12.00	8.00	17.00	13.50	45.00	3.6	3.35	55.8	51.98	4.5	4.26
33	5.24	7.00	15.00	12.50	40.00	2.13	2.10	33.03	32.61	3.13	3.06
34	14.76	7.00	15.00	12.50	40.00	2.34	2.49	36.27	38.66	3.24	3.42

Table 1 (continued)

No	Crude Loading, w/w%	pH	PEG 6000 concentration, w/w %	Sodium citrate concentration, w/w %	Temperature, °C	Purification Factor		Yield, %		Partition Coefficient, K	
						Actual	Predicted	Actual	Predicted	Actual	Predicted
35	10.00	4.62	15.00	12.50	40.00	2.36	2.09	36.58	32.40	3.26	2.98
36	10.00	9.38	15.00	12.50	40.00	2.23	2.63	34.58	40.73	3.13	3.52
37	10.00	7.00	10.24	12.50	40.00	4.09	4.08	63.38	63.27	4.99	4.98
38	10.00	7.00	19.76	12.50	40.00	3.72	3.85	57.66	59.74	4.64	4.76
39	10.00	7.00	15.00	10.12	40.00	3.16	2.77	48.98	43.00	4.06	3.66
40	10.00	7.00	15.00	14.88	40.00	2.15	2.66	33.33	41.27	3.05	3.56
41	10.00	7.00	15.00	12.50	28.11	3.55	3.48	55.03	53.98	4.45	4.39
42	10.00	7.00	15.00	12.50	51.89	3.53	3.72	54.72	57.74	4.45	4.63
43	10.00	7.00	15.00	12.50	40.00	4.11	4.60	63.72	71.30	5.03	5.50
44	10.00	7.00	15.00	12.50	40.00	4.69	4.60	72.7	71.30	5.59	5.50
45	10.00	7.00	15.00	12.50	40.00	4.33	4.60	67.13	71.30	5.25	5.50
46	10.00	7.00	15.00	12.50	40.00	4.71	4.60	73.03	71.30	5.61	5.50
47	10.00	7.00	15.00	12.50	40.00	4.73	4.60	73.32	71.30	5.63	5.50
48	10.00	7.00	15.00	12.50	40.00	4.72	4.60	73.16	71.30	5.62	5.50
49	10.00	7.00	15.00	12.50	40.00	4.69	4.60	72.69	71.30	5.59	5.50
50	10.00	7.00	15.00	12.50	40.00	4.73	4.60	73.33	71.30	5.63	5.50

Table 2 ANOVA of CCD for (a) purification factor, (b) recovery yield, % and (c) partition coefficient, K

Source	Sum of square	Degree of freedom	Mean square	*F*-value	*p*-value
Model	23.770	20	1.189	24.919	< 0.0001[a]
A	0.261	1	0.261	5.463	0.0265[a]
B	0.508	1	0.508	10.651	0.0028[a]
C	0.082	1	0.082	1.711	0.2011[b]
D	0.034	1	0.034	0.723	0.4021[b]
E	0.134	1	0.134	2.817	0.1040[b]
AB	0.008	1	0.008	0.164	0.6887[b]
AC	0.118	1	0.118	2.466	0.1272[b]
AD	0.312	1	0.312	6.543	0.0160[a]
AE	0.510	1	0.510	10.694	0.0028[a]
BC	0.938	1	0.938	19.676	0.0001[a]
BD	0.149	1	0.149	3.114	0.0882[b]
BE	0.600	1	0.600	12.570	0.0014[a]
CD	0.633	1	0.633	13.268	0.0010[a]
CE	0.005	1	0.005	0.095	0.7606[b]
DE	0.252	1	0.252	5.285	0.0289[a]
A^2	9.159	1	9.159	192.032	< 0.0001[a]
B^2	8.687	1	8.687	182.129	< 0.0001[a]
C^2	0.682	1	0.682	14.295	0.0007[a]
D^2	6.115	1	6.115	128.217	< 0.0001[a]
E^2	1.707	1	1.707	35.799	< 0.0001[a]
Residual	1.383	29	0.048		
Lack of Fit	0.995	22	0.045	0.815	0.6700[b]
Pure Error	0.388	7	0.055		
Cor Total	25.153	49			
Std. Dev	0.218				
R-Squared	0.945				
Adj R-Squared	0.907				
Pred R-Squared	0.797				
Adeq Precision	17.622				
Model	5732.299	20	286.615	25.120	< 0.0001[a]
A	65.088	1	65.088	5.704	0.0237[a]
B	125.925	1	125.925	11.036	0.0024[a]
C	21.049	1	21.049	1.845	0.1849[b]
D	7.292	1	7.292	0.639	0.4305[b]
E	30.309	1	30.309	2.656	0.1140[b]
AB	1.357	1	1.357	0.119	0.7327[b]
AC	30.323	1	30.323	2.658	0.1139[b]
AD	78.532	1	78.532	6.883	0.0137[a]
AE	118.465	1	118.465	10.383	0.0031[a]
BC	219.399	1	219.399	19.229	0.0001[a]
BD	37.997	1	37.997	3.330	0.0783[b]
BE	148.652	1	148.652	13.028	0.0011[a]
CD	156.866	1	156.866	13.748	0.0009[a]
CE	0.711	1	0.711	0.062	0.8046[b]
DE	63.647	1	63.647	5.578	0.0251[a]
A^2	2203.443	1	2203.443	193.116	< 0.0001[a]
B^2	2089.890	1	2089.890	183.164	< 0.0001[a]
C^2	165.123	1	165.123	14.472	0.0007[a]
D^2	1472.159	1	1472.159	129.024	< 0.0001[a]

Table 2 (continued)

Source	Sum of square	Degree of freedom	Mean square	*F*-value	*p*-value
E^2	411.638	1	411.638	36.077	< 0.0001[a]
Residual	330.889	29	11.410		
Lack of Fit	237.716	22	10.805	0.812	0.6722[b]
Pure Error	93.173	7	13.310		
Cor Total	6063.188	49			
Std. Dev	3.378				
R-Squared	0.945				
Adj R-Squared	0.908				
Pred R-Squared	0.798				
Adeq Precision	17.700				
Model	23.540	20	1.177	24.894	< 0.0001[a]
A	0.221	1	0.221	4.667	0.0391[a]
B	0.502	1	0.502	10.608	0.0029[a]
C	0.075	1	0.075	1.586	0.2179[b]
D	0.032	1	0.032	0.671	0.4194[b]
E	0.139	1	0.139	2.931	0.0976[b]
AB	0.012	1	0.012	0.246	0.6237[b]
AC	0.105	1	0.105	2.214	0.1476[b]
AD	0.306	1	0.306	6.476	0.0165[a]
AE	0.528	1	0.528	11.165	0.0023[a]
BC	0.949	1	0.949	20.067	0.0001[a]
BD	0.144	1	0.144	3.055	0.0911[b]
BE	0.602	1	0.602	12.738	0.0013[a]
CD	0.602	1	0.602	12.738	0.0013[a]
CE	0.006	1	0.006	0.134	0.7171[b]
DE	0.240	1	0.240	5.072	0.0321[a]
A^2	8.840	1	8.840	186.980	< 0.0001[a]
B^2	8.762	1	8.762	185.327	< 0.0001[a]
C^2	0.681	1	0.681	14.406	0.0007[a]
D^2	6.179	1	6.179	130.684	< 0.0001[a]
E^2	1.706	1	1.706	36.091	< 0.0001[a]
Residual	1.371	29	0.047		
Lack of Fit	1.011	22	0.046	0.895	0.6125[b]
Pure Error	0.360	7	0.051		
Cor Total	24.911	49			
Std. Dev	0.217				
R-Squared	0.945				
Adj R-Squared	0.907				
Pred R-Squared	0.794				
Adeq Precision	17.757				

A = Crude loading, w/w%; B = pH; C = PEG 6000 concentration, w/w %; D = Sodium citrate concentration, w/w %; E = Temperature, °C; a *p*-value less than 0.05 is significant; b *p*-value more than 0.05 is not significant

Identification of Partially Purified Bacteriocin

The SDS-PAGE profile of the purified sample, as illustrated in Fig. 2, revealed a distinct band in lane 3 corresponding to a molecular size of approximately 5.5–6.0 kDa, indicating the presence of a low-molecular-weight peptide following ATPS purification. This observation supports the successful enrichment of the target bacteriocin from the crude extract.

Further confirmation was achieved through HPLC analysis. The chromatographic profiles of crude and partially purified bacteriocin obtained via ATPS are presented in Fig. 3(a) and (b), respectively. A noticeable reduction in

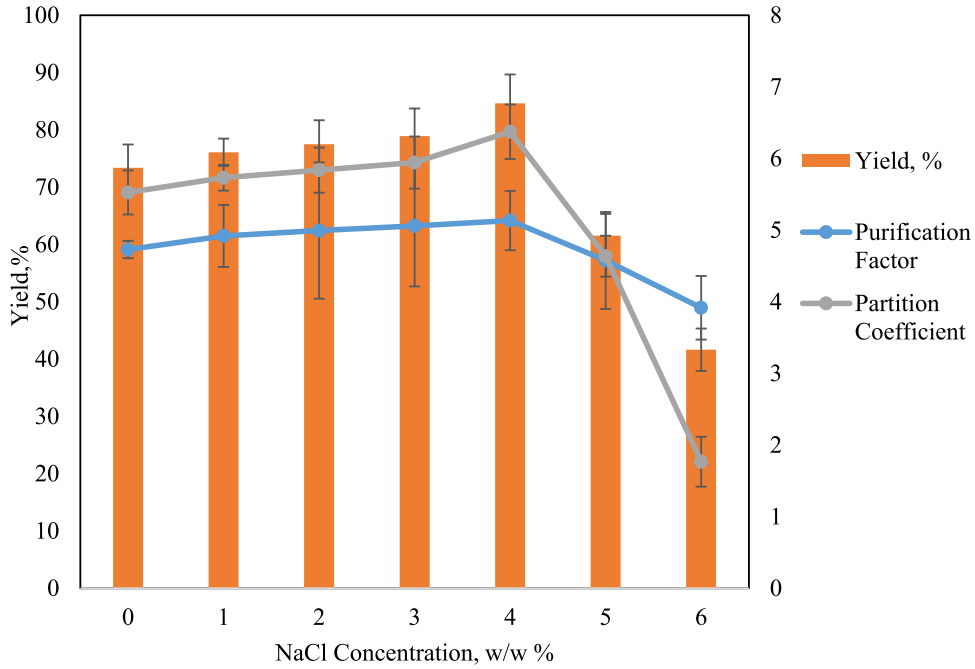

Fig. 1 Effect of NaCl on the purification factor, yield and partition coefficient of bacteriocin

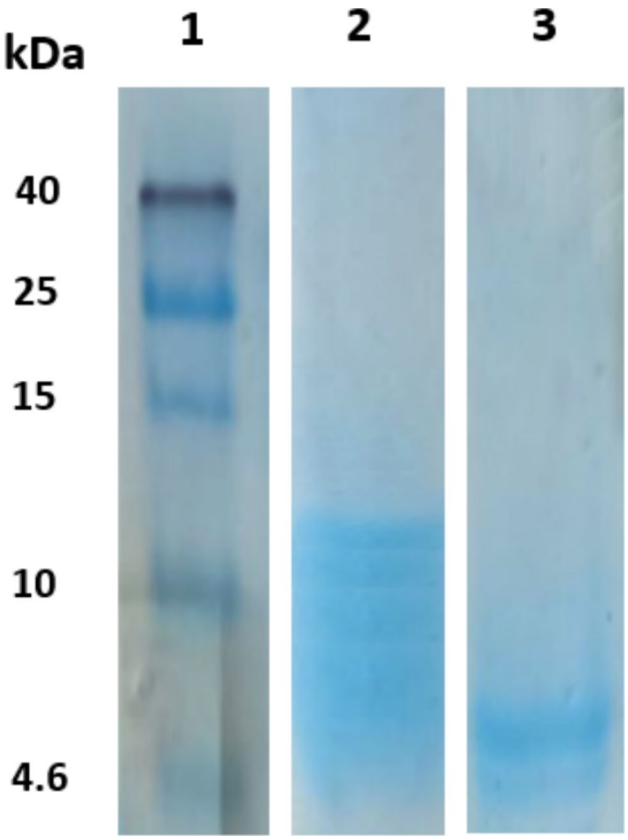

Fig. 2 SDS-PAGE protein profile. Lane 1: standard marker with molecular weight of 4.6–40 kDa. Lane 2: crude bacteriocin. Lane 3: partially purified bacteriocin by ATPS

peak complexity and intensity after purification suggests effective removal of impurities and enrichment of the bioactive component. To identify the fraction responsible for antimicrobial activity, all collected HPLC fractions were evaluated against *Streptococcus mutans* UKMCC1019 using the well diffusion assay. As shown in Table 3, two primary peaks were detected, with Fraction 2—eluting at a retention time of 17.232 min—demonstrating the highest antimicrobial activity at 1426.99 ± 140.59 AU/mL. This fraction was collected and lyophilized for further molecular characterization.

Ion trap mass spectrometry (MS) analysis of the active fraction (Fig. 4) revealed a precursor ion at m/z 707.90, corresponding to a doubly charged peptide with a protonated molecular mass of 1413.76 Da, eluting at a retention time of 32.20 min. The deduced amino acid sequence, IIGNNAAANLTTGGK, showed 71% identity with enterocin HF (UniProt Primary Accession: P86183). Based on its distinct sequence and physicochemical characteristics, the peptide was designated as a novel enterocin and named enterocin CC2. This integrated identification strategy confirms the successful purification and preliminary structural characterization of a unique bacteriocin with promising antimicrobial activity against oral pathogens.

Antimicrobial Activity of Partially Purified Enterocin CC2 against *S. mutans* UKMCC1019

The MIC and MBC of partially purified enterocin CC2 were evaluated against *S. mutans* UKMCC1019. As shown in Fig. 5 (a), the inhibition of *S. mutans* UKMCC1019 increased with increasing concentrations of partially purified

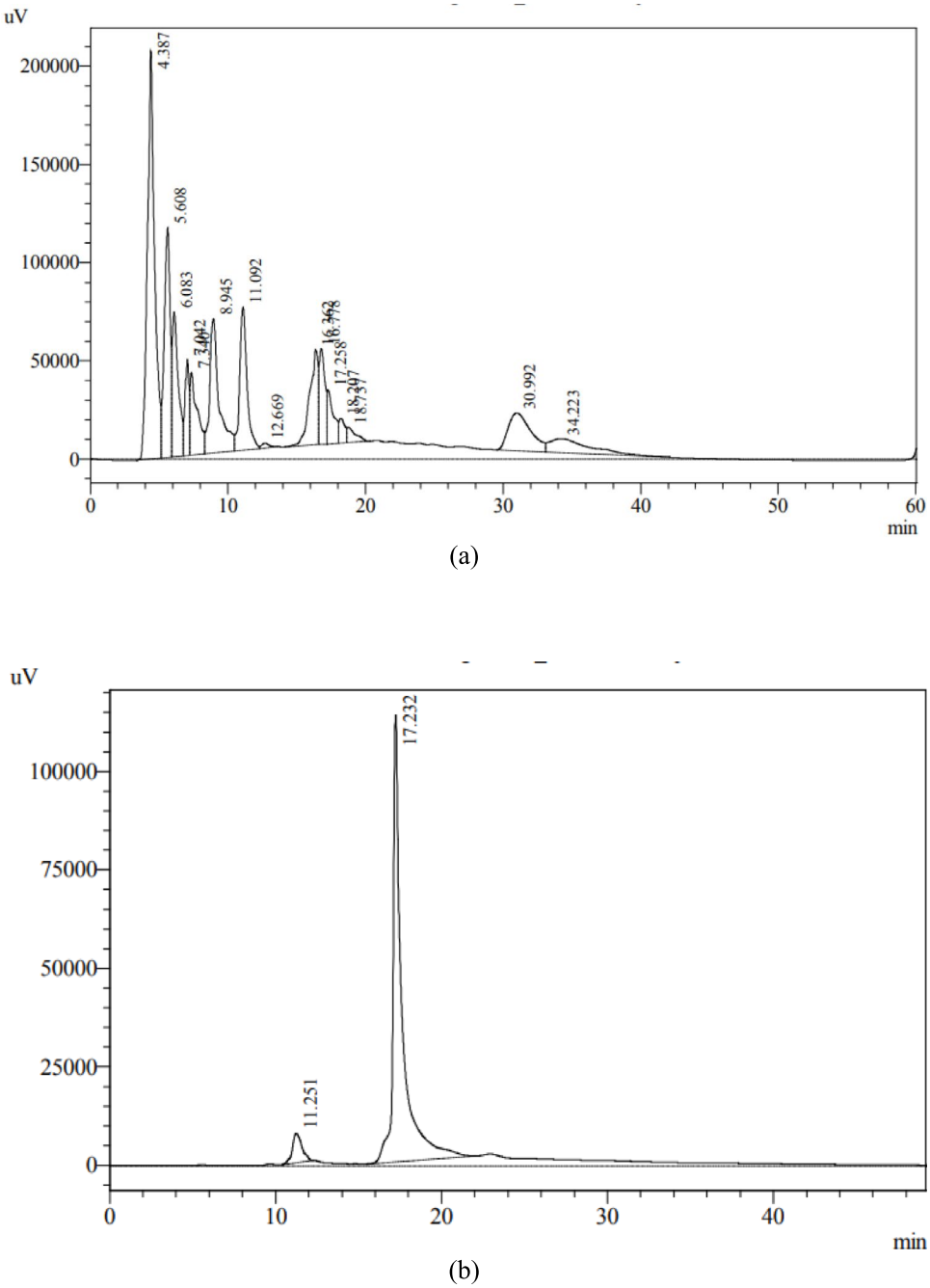

Fig. 3 HPLC analysis chromatogram of (**a**) crude bacteriocin and (**b**) partially purified bacteriocin by ATPS

Table 3 Inhibition activity of different fractions against *S. mutans* UKMCC1019

Fractions	Retention time, min	Inhibition Activity, (mean ± standard deviation) AU/ml
1	11.251	0
2	17.232	1426.99 ± 140.59

bacteriocin. At 0.125 mg/mL, bacterial growth was inhibited by more than 50%, while complete inhibition was achieved at an MIC of 0.500 mg/mL.

Similarly, Fig. 5 (b) illustrates the MBC of partially purified enterocin CC2, demonstrating a significant reduction in the viable cell count of *S. mutans* UKMCC1019 as the bacteriocin concentration increased. The MBC was determined to be 1.00 mg/mL, where no viable bacterial cells were detected. These values demonstrate strong antimicrobial potency, emphasizing its translational potential as a therapeutic candidate for oral infections.

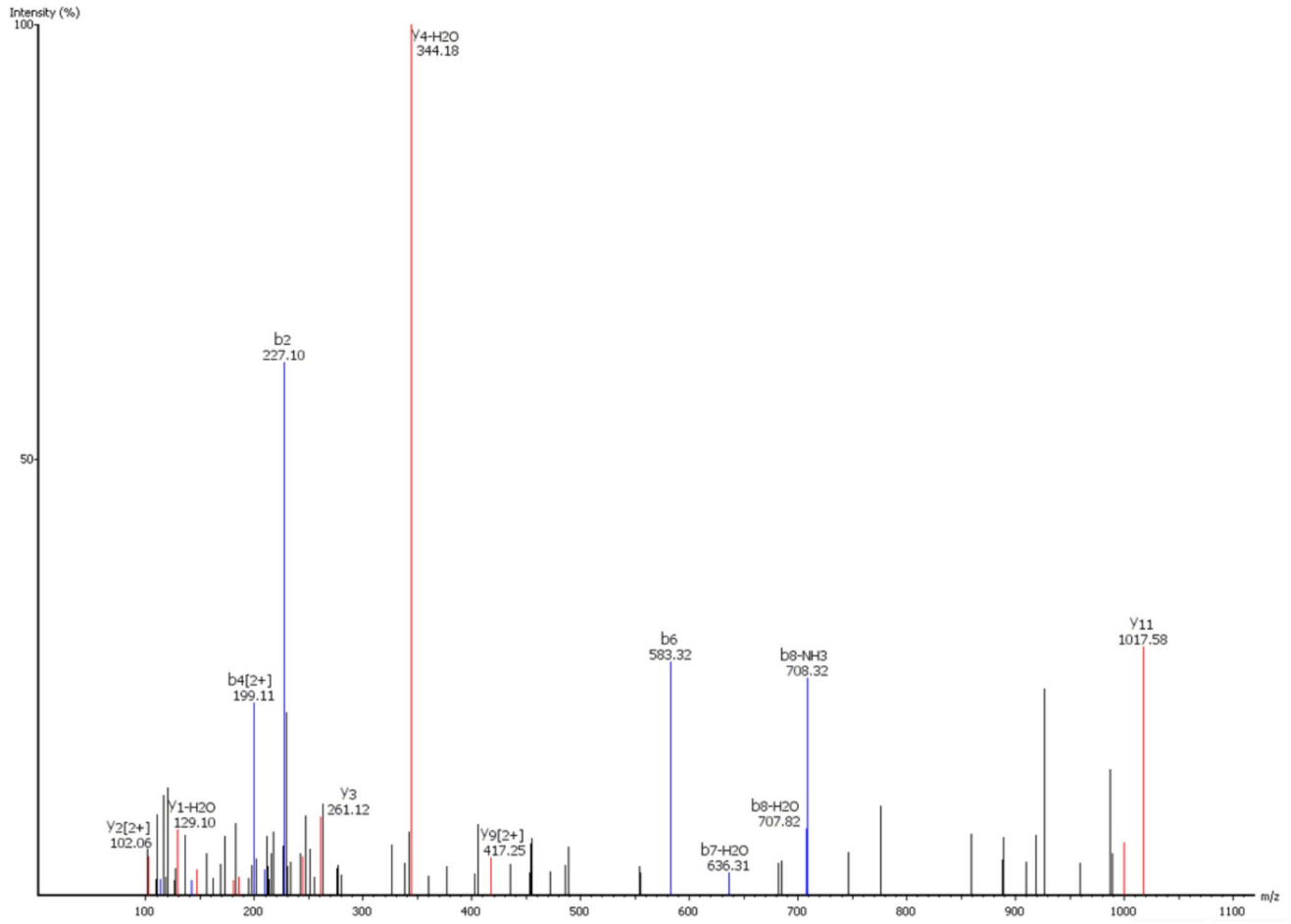

Fig. 4 Ion Trap MS mass spectrum of the peptide IIGNNAAANLTTGGK assigned to the enterocin CC2 (precursor m/z: 707.90 Da; protonated mass = 1413.76 Da; charge Z = + 2; retention time = 32.20 min)

Growth Curve and Time-kill Kinetics Assays for *S. mutans* UKMCC1019 Treated with Partially Purified Enterocin CC2

Figure 6 (a) illustrates the growth curve of *S. mutans* UKMCC1019 treated with 0.500 mg/mL of partially purified bacteriocin, 0.2% chlorhexidine (positive control), and untreated bacteria (negative control). The results indicate that 0.500 mg/mL of partially purified bacteriocin significantly inhibited the growth of *S. mutans* UKMCC1019 compared to the negative control. Notably, the antimicrobial effect of partially purified bacteriocin exceeded that of the positive control (0.2% chlorhexidine), demonstrating its superior inhibitory potential.

Figure 6 (b) presents the time-kill kinetics of partially purified bacteriocin against *S. mutans* UKMCC1019 at concentrations of 1-, 2-, and fourfold of the MBC. The results confirm that bacteriocin exhibited bactericidal activity in a dose- and time-dependent manner. The time required for complete bacterial eradication at 1-, 2-, and fourfold MBC concentrations was 8 h, 4.5 h, and 2 h, respectively. In contrast, 0.2% chlorhexidine required 11 h for complete bacterial elimination, indicating that partially purified bacteriocin achieved faster bacterial clearance. These findings highlight the potential of enterocin CC2 as an effective and rapid antimicrobial agent against *S. mutans* UKMCC1019, surpassing the efficacy of conventional chlorhexidine treatment.

Cytotoxicity Test

The cytotoxicity of the partially purified enterocin CC2 was evaluated using the 3T3-L1 fibroblast cell line, as illustrated in Fig. 7. Cell viability was assessed following exposure to varying concentrations of the peptide. According to ISO 10993–5 guidelines, a reduction in cell viability exceeding 30% is indicative of cytotoxicity.

The results demonstrated that enterocin CC2 at concentrations of 1.00 mg/mL and below maintained cell viability

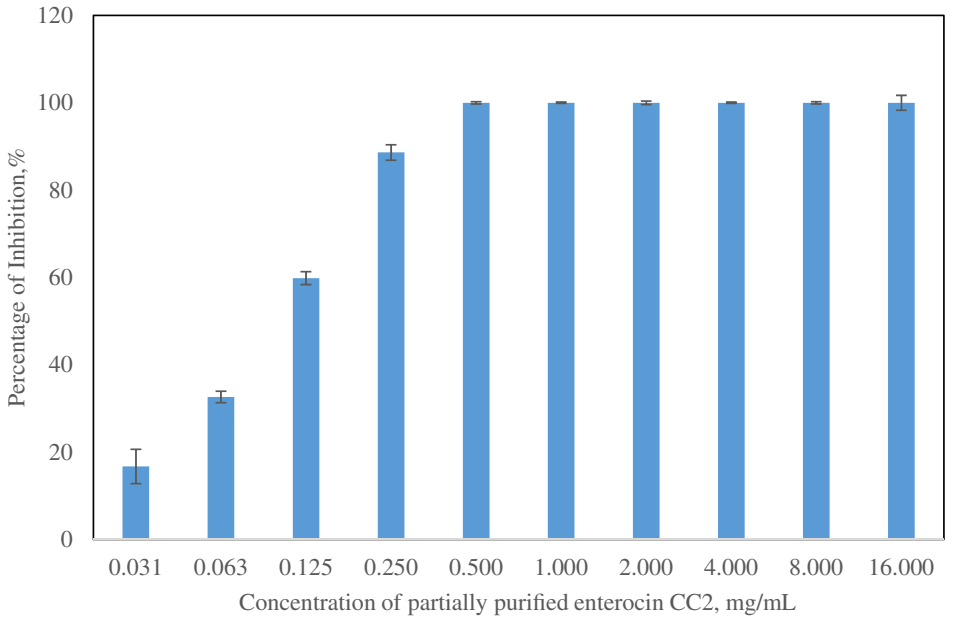

(a)

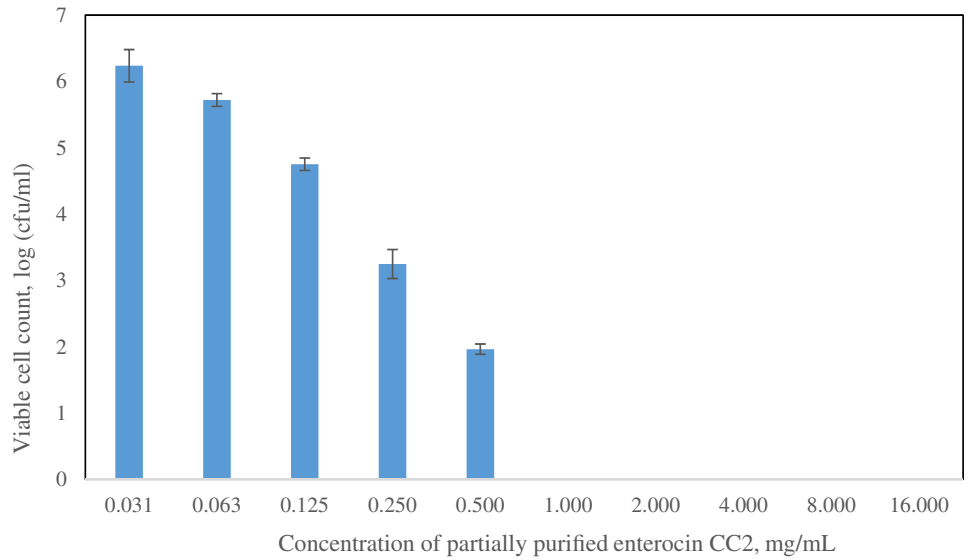

(b)

Fig. 5 **a** The minimum inhibitory concentration (MIC) and (b) minimum bactericidal concentration (MBC) of partially purified enterocin CC2 against *S. mutans* UKMCC1019

above the cytotoxicity threshold, indicating a favourable safety profile at these levels. However, at 2.00 mg/mL, a significant decline in viability was observed, suggesting potential cytotoxic effects at higher concentrations. These findings highlight that enterocin CC2 exerts no apparent cytotoxicity within its effective antimicrobial range, supporting its potential for safe application in oral therapeutics.

Conclusion

This study successfully demonstrated the sustainable bioprocessing and therapeutic promise of enterocin CC2, a probiotic-derived antimicrobial peptide produced by *Enterococcus faecium* CC2. A polyethylene glycol (PEG)-based aqueous two-phase system (ATPS) was systematically optimized to achieve high purification efficiency under mild and scalable conditions, yielding a purification factor of 4.73, recovery yield of 73.33%, and partition coefficient of 5.63. The addition of 4% NaCl further enhanced these

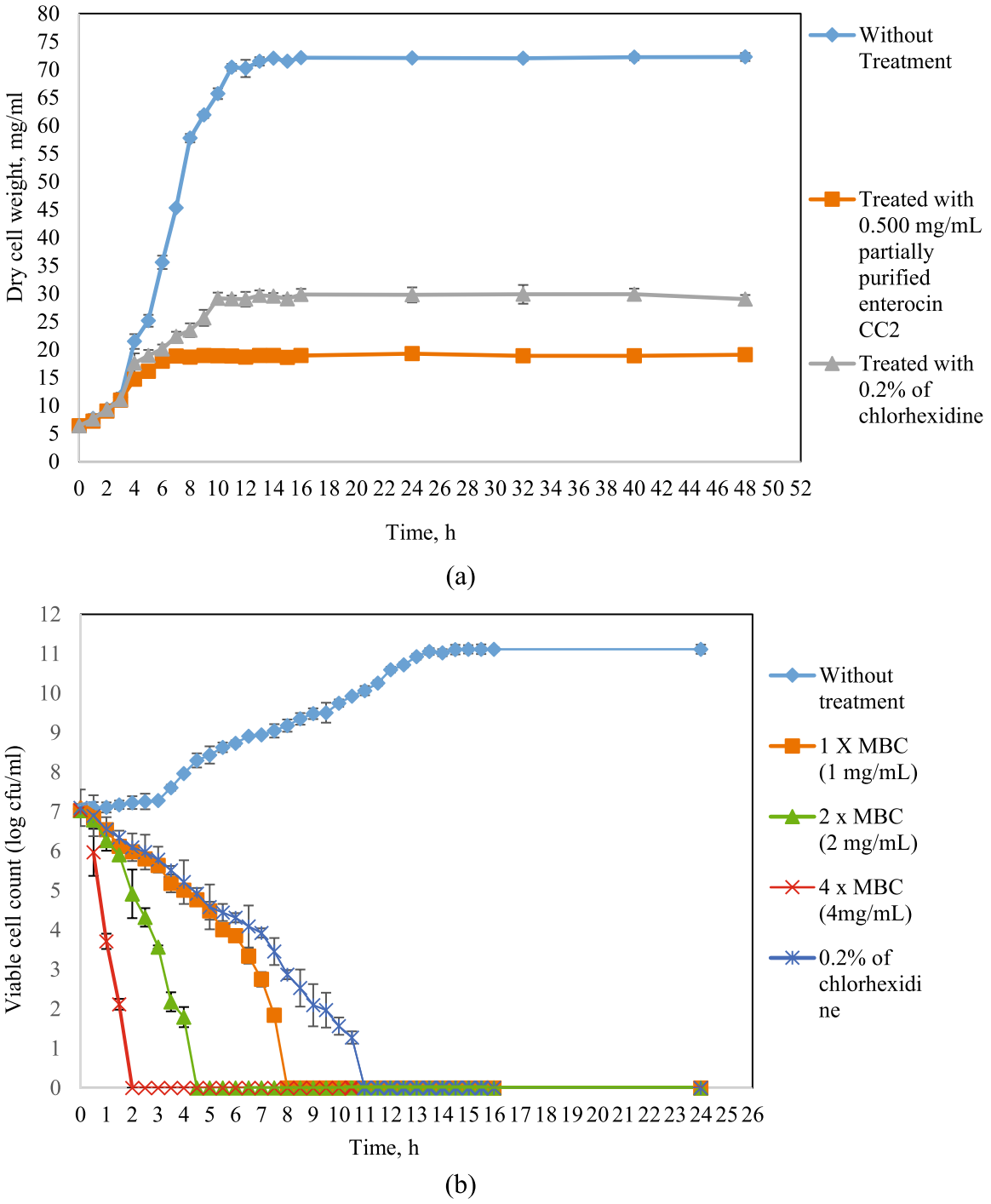

Fig. 6 **a** Growth curve and (**b**) time-kill kinetics for *S. mutans* UKMCC1019 treated with partially purified enterocin CC2

metrics to 5.13, 84.61%, and 6.37, respectively, surpassing values reported for ionic liquid-based systems. The partially purified enterocin CC2 exhibited a molecular weight of ~ 5.5–6.0 kDa and was confirmed via HPLC and LC–MS/MS to share 71% sequence identity with enterocin HF, supporting its novelty. The peptide displayed potent inhibitory activity against *Streptococcus mutans* UKMCC1019, with MIC and MBC values of 0.50 mg/mL and 1.00 mg/mL, respectively. Time-kill kinetics further revealed rapid bactericidal action exceeding that of 0.2%

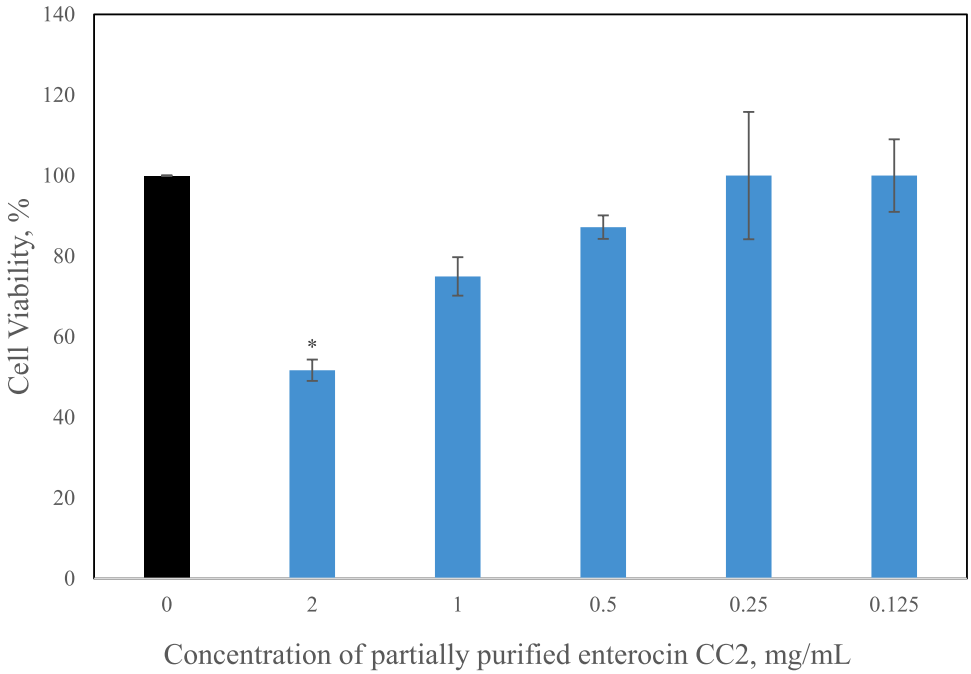

Fig. 7 The effect of different concentration of partially purified enterocin on the 3T3-L1 cell viability. Results are shown as Mean ± SD with $p \leq 0.05$ are considered significant

chlorhexidine. Importantly, cytotoxicity assays confirmed its safety profile, showing no adverse effects on 3T3-L1 cells at concentrations ≤ 1.00 mg/mL. Collectively, the potent antimicrobial activity and favourable safety profile of enterocin CC2 highlight its potential for incorporation into oral care formulations such as mouth rinses, sprays, gels, or varnishes designed to reduce cariogenic bacterial load. From an environmental and industrial perspective, the PEG–citrate ATPS developed here offers a sustainable and eco-friendly purification strategy. Both PEG and citrate are biocompatible, food-grade, and recyclable components, making this approach more suitable for early industrial application compared with ionic liquid-based systems. The mild operating conditions and cost-effective inputs further strengthen its scalability as a practical downstream platform for probiotic-derived antimicrobials, advancing the translational development of bacteriocin-based therapeutics for oral health. Nevertheless, certain limitations should be acknowledged. Antimicrobial evaluation was restricted to a single *S. mutans* strain, and broader testing against multiple oral pathogens and complex biofilm models is required. In addition, cytotoxicity assessment was limited to one fibroblast cell line; therefore, future studies involving oral epithelial cells and in vivo validation will be essential to comprehensively establish biosafety and therapeutic applicability. Beyond these immediate limitations, future research should also focus on optimizing enterocin CC2 for incorporation into practical oral care formulations such as rinses, sprays, gels, or varnishes, and on evaluating its stability under storage and salivary conditions. Exploring synergistic effects with existing agents like fluoride or probiotics could further enhance efficacy. In parallel, pilot-scale production and cost-effectiveness studies will be important to support industrial feasibility and accelerate clinical translation.

Supplementary Information The online version contains supplementary material available at https://doi.org/10.1007/s12602-025-10773-2.

Acknowledgements The author (Ng Zhang Jin) would like to express his great appreciation and gratitude to Universiti Sains Malaysia for hiring him as USM Postdoctoral fellow.

Author Contribution Author 1: Zhang Jin Ng Contribution: Methodology, Investigation, Data curation, Formal analysis, Writing – original draft Author 2: Chee-Yuen Gan Contribution: Data curation, Formal analysis Author 3: Mazni Abu Zarin Contribution: Data curation, Validation Author 4: Chee Keong Lee Contribution: Validation, Supervision Author 5: John Chi-Wei Lan Contribution: Writing – review & editing Author 6: Hui Suan Ng Contribution: Writing – review & editing Author 7:Joo Shun Tan Contribution: Conceptualization, Supervision, Writing – review & editing.

Funding Open access funding provided by The Ministry of Higher Education Malaysia and Universiti Sains Malaysia. Authors acknowledge the financial supports received by Ministry of Higher Education (MOHE), Malaysia under Fundamental Research Grant Scheme [FRGS/1/2022/STG01/USM/02/21].

Data Availability No datasets were generated or analysed during the current study.

Declarations

Conflict of Interest The authors declare no competing interests.

References

1. Abdul Aziz NFH, Abbasiliasi S, Ng ZJ, Abu Zarin M, Oslan SN, Tan JS, Ariff AB (2020) Recovery of a bacteriocin-like inhibitory substance from *Lactobacillus bulgaricus* FTDC 1211 using polyethylene-glycol impregnated amberlite XAD-4 resins system. Molecules. https://doi.org/10.3390/molecules25225332
2. Atta L, Siddiqui AR, Mushtaq M, Munsif S, Nur-e-Alam M, Ahmed A, Ul-Haq Z (2025) Molecular insights into antibiofilm inhibitors of *Streptococcus mutans* glucosyltransferases through in silico approaches. Sci Rep 15(1):14160. https://doi.org/10.1038/s41598-025-98927-8
3. Aziz T, Hangyu H, Naveed M, Shabbir MA, Sarwar A, Nasbeeb J, Zhennai Y, Alharbi M (2024) Genotypic profiling, functional analysis, cholesterol-lowering ability, and Angiotensin I-converting enzyme (ACE) inhibitory activity of probiotic *Lactiplantibacillus plantarum* K25 via different approaches. Probiotics Antimicrob Proteins. https://doi.org/10.1007/s12602-024-10258-8
4. Aziz T, Naveed M, Shabbir MA, Naseeb J, Sarwar A, Zhao L, Yang Z, Haiying C, Lin L, Shami A, Al-Asmari F (2025) Genomic profiling of *Pediococcus acidilactici* BCB1H and identification of its key features for biotechnological innovation, food technology and medicine. Sci Rep 15(1):6050. https://doi.org/10.1038/s41598-025-90633-9
5. Aziz T, Shabbir MA, Sarwar A, Khan AA, Zhao L, Yang Z, Shami A, Alwethaynani MS, Al-Asmari F, Alghamdi AM, Al-Joufi FA (2025) Exploring the multifaceted probiotic potential of *Lactiplantibacillus plantarum* NMGL2, investigating its antimicrobial resistance profiles and bacteriocin production. J Microbiol Methods 236:107178. https://doi.org/10.1016/j.mimet.2025.107178
6. Bekavac N, Benković M, Jurina T, Valinger D, Gajdoš Kljusurić J, Jurinjak Tušek A, Šalić A (2024) Advancements in aqueous two-phase systems for enzyme extraction, purification, and biotransformation. Molecules. https://doi.org/10.3390/molecules29163776
7. Bloch S, Hager-Mair FF, Andrukhov O, Schäffer C (2024) Oral streptococci: modulators of health and disease. Front Cell Infect Microbiol. https://doi.org/10.3389/fcimb.2024.1357631
8. Chen Y, Huang Y, Lin H, Chen D (2024) The effects and mechanisms of novel antibacterial amyloid peptides derived from *Streptococcus mutans* proteome. Chem Eng J 497:154458. https://doi.org/10.1016/j.cej.2024.154458
9. Eydou Z, Jad BN, Elsayed Z, Ismail A, Magaogao M, Hossain A (2020) Investigation on the effect of vitamin C on growth & biofilm-forming potential of *Streptococcus mutans* isolated from patients with dental caries. BMC Microbiol 20(1):231. https://doi.org/10.1186/s12866-020-01914-4
10. Hebling, J., Bianchi, L., Basso, F. G., Scheffel, D. L., Soares, D. G., Carrilho, M. R., . . . de Souza Costa, C. A. (2015). Cytotoxicity of dimethyl sulfoxide (DMSO) in direct contact with odontoblast-like cells. *Dent Mater, 31*(4), 399–405. https://doi.org/10.1016/j.dental.2015.01.007
11. Janković T, Straathof AJ, Kiss AA (2024) A perspective on downstream processing performance for recovery of bioalcohols. J Chem Technol Biotechnol 99(9):1933–1940. https://doi.org/10.1002/jctb.7690
12. Kee PE, Lan JC, Yim HS, Tan JS, Chow YH, Ng HS (2020) Efficiency of ionic liquids-based aqueous two-phase electrophoresis for partition of Cytochrome c. Appl Biochem Biotechnol 191(1):376–386. https://doi.org/10.1007/s12010-019-03202-y
13. Lau BYC, Othman A (2019) Evaluation of sodium deoxycholate as solubilization buffer for oil palm proteomics analysis. PLoS ONE 14(8):e0221052. https://doi.org/10.1371/journal.pone.0221052
14. Li Y, Huang S, Du J, Wu M, Huang X (2023) Current and prospective therapeutic strategies: tackling *Candida albicans* and *Streptococcus mutans* cross-kingdom biofilm. Front Cell Infect Microbiol. https://doi.org/10.3389/fcimb.2023.1106231
15. Liu G, Nie R, Liu Y, Mehmood A (2022) Combined antimicrobial effect of bacteriocins with other hurdles of physicochemic and microbiome to prolong shelf life of food: a review. Sci Total Environ 825:154058. https://doi.org/10.1016/j.scitotenv.2022.154058
16. Mahale VD, Sharma S (2024) Evaluation of minimum inhibitory concentration and minimum bactericidal concentration of royal jelly against *Enterococcus faecalis*, *Staphylococcus aureus*, and *Candida albicans*. J Conserv Dent Endod 27(3):252–256. https://doi.org/10.4103/jcde.Jcde_234_23
17. Ng ZJ, Zarin MA, Lee CK, Phapugrangkul P, Tan JS (2020) Isolation and characterization of *Enterococcus faecium* DSM 20477 with ability to secrete antimicrobial substance for the inhibition of oral pathogen *Streptococcus mutans* UKMCC 1019. Arch Oral Biol 110:104617. https://doi.org/10.1016/j.archoralbio.2019.104617
18. Pingitore EV, Salvucci E, Sesma F, Nader-Macias ME (2007) Different strategies for purification of antimicrobial peptides from Lactic Acid Bacteria (LAB). Communicat Curr Res Educ Topic Trend Appl Microbiol 2007(1):557–68
19. Salam MA, Al-Amin MY, Salam MT, Pawar JS, Akhter N, Rabaan AA, Alqumber MAA (2023) Antimicrobial resistance: a growing serious threat for global public health. Healthcare. https://doi.org/10.3390/healthcare11131946
20. Santos AG, Buarque FS, Ribeiro BD, Coelho MAZ (2022) Extractive fermentation for the production and partitioning of lipase and citric acid by *Yarrowia lipolytica*. Process Biochem 122:374–385. https://doi.org/10.1016/j.procbio.2022.09.011
21. Shah SAR, Hussan S, Ben Kahla N, Anwar MK, Baluch MA, Nawaz A (2024) Performance evaluation and optimization of binder-toner and mixing efficiency ratios in an e-waste toner-modified composite mixture using response surface methodology. Infrastructures 9(11):200
22. Spatafora G, Li Y, He X, Cowan A, Tanner ACR (2024) The evolving microbiome of dental caries. Microorganisms 12(1):121
23. van Tonder A, Joubert AM, Cromarty AD (2015) Limitations of the 3-(4,5-dimethylthiazol-2-yl)-2,5-diphenyl-2H-tetrazolium bromide (MTT) assay when compared to three commonly used cell enumeration assays. BMC Res Notes 8(1):47. https://doi.org/10.1186/s13104-015-1000-8
24. Zhang X, Han M, Han S, Zong W (2025) Aqueous two-phase system (ATPS): from basic science to applications. RSC Adv 15(12):9041–9054. https://doi.org/10.1039/D4RA08232J
25. Zore A, Rojko F, Mlinarić NM, Veber J, Učakar A, Štukelj R, Pondelak A, Sever Škapin A, Bohinc K (2024) Effect of sucrose concentration on *Streptococcus mutans* adhesion to dental material surfaces. Coatings 14(2):165